Journal of Energy Storage

Multi-objective identification of a metal hydride tank model

--Manuscript Draft--

Manuscript Number:	EST-D-25-01733
Article Type:	VSI: HYCELTEC2024
Keywords:	Metal hydride tanks; Mathematical model; Identifiability analysis; Sensitivity analysis; Multi-objective optimisation
Corresponding Author:	Ramon Costa-Castelló, Ph.D. Polytechnic University of Catalonia SPAIN
First Author:	Mingrui Chen
Order of Authors:	Mingrui Chen
	Carles Batlle Arnau
	Bryan Escachx Estevez
	Ramon Costa-Castelló
	Jing Na
Abstract:	In this paper, a three-dimensional state-space model of the metal hydride tank is formulated and analysed. Before the identification of the unknown parameters of the model, we first analysed their identifiability, i.e., whether we can obtain a unique unknown parameter vector from the available information. Secondly, due to the large number of unknown parameters in the proposed model, the identification of all the unknown parameters requires huge computational costs. In order to reduce the number of unknown parameters that need to be identified, we performed a sensitivity analysis of unknown parameters for the developed model. Finally, since the model has two outputs, we performed single-objective and multi-objective identification on the same experimental data, and the results show that multi-objective identification is more effective.

Highlights

- A three-dimensional state-space model of the MH tank is formulated and analysed.
- Identifiability analysis and sensitivity analysis for the MH tank model.
- Calibrate the unknown parameters in the model based on experimental data using multi-objective identification methods.

Declaration of interests

☒The authors declare that they have no known competing financial interests or personal relationships that could have appeared to influence the work reported in this paper.

☐The authors declare the following financial interests/personal relationships which may be considered as potential competing interests:

Multi-objective identification of a metal hydride tank model

Mingrui Chen[a], Carles Batlle[b], Bryan Escachx[a], Ramon Costa-Castelló[c,*] and Jing Na[c,d]

[a]Institut de Robòtica i Informàtica Industrial, CSIC-UPC. C/ Llorens i Artigas 4-6, 08028 Barcelona, Spain
[b]Departament de Matemàtiques, Institut d'Organització i Control, EPSEVG, UPC, 08800 Vilanova i la Geltru, Spain
[c]Universitat Politècnica de Catalunya, Avinguda Diagonal, 647, 08028 Barcelona, Spain
[d]Faculty of Mechanical and Electrical Engineering, Kunming University of Science and Technology, Kunming, 650500, PR China
[e]Yunnan Key Laboratory of Intelligent Control and Application, Kunming, 650500, PR China

ARTICLE INFO

Keywords:
Metal hydride tanks
Mathematical model
Identifiability analysis
Sensitivity analysis
Multi-objective optimisation

ABSTRACT

In this paper, a three-dimensional state-space model of the metal hydride tank is formulated and analysed. Before the identification of the unknown parameters of the model, we first analysed their identifiability, i.e., whether we can obtain a unique unknown parameter vector from the available information. Secondly, due to the large number of unknown parameters in the proposed model, the identification of all the unknown parameters requires huge computational costs. In order to reduce the number of unknown parameters that need to be identified, we performed a sensitivity analysis of unknown parameters for the developed model. Finally, since the model has two outputs, we performed single-objective and multi-objective identification on the same experimental data, and the results show that multi-objective identification is more effective.

1. Introduction

The metal hydride (MH) tank, a widely used container for solid-state hydrogen storage, has been modelled and studied since the 1980s. The chemical reaction between MH and hydrogen can be expressed as the following equation.

$$M + \frac{x}{2}H_2 \underset{\text{desorption}}{\overset{\text{absorption}}{\leftrightarrow}} MH_x + \Delta H, \tag{1}$$

where M is the metal alloy, MH_x is the metal hydride and ΔH is the reaction heat. Suda et al. [30] investigated the reaction kinetics of alloys such as $LaNi_5$ during the adsorption and desorption process and modelled the reaction rate constants for these two processes using two functions. At the same time, they found that mixing increases the number of metal hydrides and improves the reaction kinetics. Mayer et al. [19] studied the heat and mass transfer properties of metal hydride reaction beds and established a corresponding model. The established model is consistent with the experimental results, so the model can be used to predict the kinetic behaviour of the reaction bed. Besides, the Van't Hoff equation was used for the calculation of equilibrium pressure. Subsequently, the heat and mass transfer modelling of metal hydride storage tanks of different shapes and different materials has been intensively investigated by many researchers [1, 6].

In these different models established, there exist a number of unknown parameters. For the unknown parameters of a system, it is possible to estimate their values by measuring the system's inputs and outputs through identification techniques. However, this leads to a fundamental question: can a unique set of unknown parameters be determined solely based on the given inputs and outputs? Addressing this issue requires solving the identifiability problem, which assesses whether the model structure permits a unique parameter solution under the provided data. Identifiability can be categorised into point identifiability and structural identifiability [26]. Structural identifiability methods can be used for models with less than 10 states and parameters [26]. For models with more states and parameters, local point identifiability is the only approach. Point identifiability analysis is mainly based on the sensitivity of the model's output. From the point of view of output sensitivity, a larger output change caused by the same percentage of system parameter change indicates that this parameter has a larger output sensitivity. Therefore, if the system output has a high sensitivity for a small variation of a parameter, then it is more likely that the parameter can be recovered based on the output information, i.e. this parameter is likely to be identifiable. The matrix composed of the output sensitivity coefficients of each parameter is the output sensitivity matrix [20]. Jacquez et al. [14] proposed the correlation method; They used the linearization in parameter space around the prespecified value to check the local identifiability and judge whether the parameters are distinguishable from each other based on the column correlation of the sensitivity matrix. Yue et al. [33] proposed the orthogonal method and a forward selection algorithm is used to analyse the identifiability of the parameters. Besides, there is also the eigenvalue method proposed by Vajda et al. [31], the tuning importance method [12], among others.

After determining that the parameters are identifiable, the unknown parameters can be identified based on the system output. Small variations in each unknown parameter can affect the system output differently, so sensitivity analysis of the unknown parameters in the system is required to determine the effect of each parameter on the system output, thus reducing the number of parameters that need to be identified. Christopher et al. [8] classified sensitivity analysis

*Corresponding author
chenmingrui2018@gmail.com (M. Chen); carles.batlle@upc.edu (C. Batlle); bryan.escachx@upc.edu (B. Escachx); ramon.costa@upc.edu (R. Costa-Castelló); najing25@163.com (J. Na)

methods into 3 main categories: mathematical, statistical and graphical methods; They selected 10 different sensitivity analysis methods and analysed them in comparison with some criteria. Choi et al. [7] used Multi-Parametric Sensitivity Analysis (MPSA) to analyse the relative importance of factors influencing the natural attenuation of mining contaminants. Similarly, Correa et al. [10] used MPSA to analyse parameter sensitivity in the Proton Exchange Membrane Fuel Cell (PEMFC) model. MPSA requires the determination of nominal parameters and a large number of Monte Carlo simulations are needed to perform the analysis, which can be time-consuming when the number of parameters is large. Benchluch et al. [3] used the trajectory sensitivity technique to analyse the parameter sensitivity of nonlinear excitation system models. This method does not require linearization of the model and can be used to obtain the sensitivity directly from the nonlinear model. For MH tanks, Suarez et al. [29] investigated the sensitivity of three parameters of the MH tank model that change significantly from a healthy to a degraded state. Xiao et al. [32] proposed a new multi-parameter sensitivity analysis method, which is based on the Latin hypercube sampling and the rank correlation method, then they investigated the sensitivity ranking of 10 parameters in the pressure-composition-temperature (PCT) curve model according to this new sensitivity analysis method.

After obtaining the results of the analysis of parameter sensitivity, the unknown parameters of the model need to be identified. For systems with only a single output, it is sufficient to use a single objective function, but for systems with multiple outputs, not all outputs might be fitted simultaneously due to structural uncertainty. Besides, for contradictory multiple objectives, the use of single objective optimisation methods is also inappropriate. Therefore, multi-objective optimisation methods are needed. Qian et al. [25] designed the shape of the wind-to-heat system blades using multi-objective optimisation based on the Particle Swarm Optimisation (PSO) algorithm and compared it with single objective optimisation. Nyamsi et al. [24] presented a multi-objective optimisation approach to minimise the hydrogen absorption/desorption time of the MH tanks, where the optimal solution was selected on a Pareto front.

The objective of this paper is to develop a state-space model of the MH tank and to analyse the identifiability and sensitivity of the unknown parameters in this model. Based on the experimental data, a multi-objective optimisation method is used to identify the unknown parameters in the model. The paper is organized as follows: Section 2 presents a three-dimensional state-space model of the MH tank. Section 3 analyses the parameter identifiability of the MH tank model using the correlation method. In Section 4, the First-order Trajectory Sensitivity Analysis (FOTSA) method is used to analyse the parameter sensitivity for the proposed MH tank model. Section 5 identifies the unknown parameters in the model using the PSO algorithm and the paretosearch algorithm for single and multi-objective identification and compares the results of the two identification methods. Finally, the conclusions and future work are provided in Section 6.

2. Model of the MH tank

In previous literature [15], a three-dimensional state-space model of the MH tank was proposed, which took the temperature of the MH tank as a system state and considered the effect of the external cooling circulation. This model is suitable for the thermal management of the MH tank, but it is slightly complex for cases where the heat exchange between the tank and the external environment does not need to be considered. In this section, we simplify the model presented in [15] and modify the simplified model based on the inputs of the experimental setup.

2.1. Mass Balance

The mass balance for hydrogen can be expressed as:

$$\frac{\mathrm{d}\rho_{\mathrm{g}}}{\mathrm{dt}} = \frac{m'_{in} - m'_r}{v_t - v_{MH} \cdot (1-\varepsilon)}, \tag{2}$$

where ρ_g denotes the hydrogen density, m'_{in} represents the mass flow rate of hydrogen entering or leaving the tank, and m'_r corresponds to the rate of hydrogen absorption or desorption. The parameters v_t and v_{MH} are the tank volume and the volume of the metal hydride, respectively, while ε indicates the porosity of the metal hydride. In this equation, the numerator represents the time rate of change of hydrogen mass, and the denominator reflects the total volume of hydrogen within the tank.

Introducing normalized parameters: the mass-flow rate of hydrogen, $f_{in} \triangleq m'_{in}/v_{MH}$; the normalized sorption mass-flow rate, $f_r \triangleq m'_r/v_{MH}$; and the normalized hydrogen volume, $v_g \triangleq v_t/v_{MH} - 1 + \varepsilon$. Eq. (2) is then reformulated as:

$$\frac{\mathrm{d}\rho_{\mathrm{g}}}{\mathrm{dt}} = \frac{f_{in} - f_r}{v_g}. \tag{3}$$

For the metal hydride, a similar mass balance gives:

$$\frac{\mathrm{d}\rho_{\mathrm{s}}}{\mathrm{dt}} = \frac{m'_r}{v_{MH} \cdot (1-\varepsilon)}, \tag{4}$$

where ρ_s is the density of the metal hydride. The denominator here represents the effective volume of the metal hydride within the tank. Defining the normalized volume of the metal hydride as $v_s \triangleq 1-\varepsilon$, Eq. (4) simplifies to:

$$\frac{\mathrm{d}\rho_{\mathrm{s}}}{\mathrm{dt}} = \frac{f_r}{v_s}. \tag{5}$$

2.2. Reaction Kinetics

The normalized sorption mass-flow rate, f_r, is not directly measurable. A commonly adopted model [18] is described as follows:

$$f_r = \begin{cases} c_a e^{-\frac{E_a}{R \cdot T_t}} \ln\left(\frac{p}{p_{eq,a}}\right)(\rho_{ss} - \rho_s), & p > p_{eq,a}, \quad (6a) \\ c_d e^{-\frac{E_d}{R \cdot T_t}} \left(\frac{p - p_{eq,d}}{p_{eq,d}}\right)(\rho_s - \rho_{s0}), & p < p_{eq,d}, \quad (6b) \\ 0, & \text{otherwise.} \quad (6c) \end{cases}$$

Here, c_a and c_d are absorption and desorption constants, E_a and E_d are activation energies, R is the universal gas constant, and T_t represents the tank temperature. The equilibrium pressures for absorption and desorption are $p_{eq,a}$ and $p_{eq,d}$, respectively. The terms $c_a e^{-E_a/(RT_t)}$ and $c_d e^{-E_d/(RT_t)}$ are rate coefficients derived using the Arrhenius equation [23]. The parameter ρ_{ss} denotes the saturation density of the metal hydride, while ρ_{s0} is the density of the bare metal alloy (without hydrogen).

The MH tank pressure p is assumed to follow the ideal gas law:

$$p = \rho_g \frac{T_t R}{M_{H_2}}, \tag{7}$$

where M_{H_2} is the molar mass of hydrogen.

The saturation density, ρ_{ss}, can be calculated as:

$$\rho_{ss} = \rho_{s0} + \frac{\upsilon_{H_2} \cdot \rho_{H_2}}{\upsilon_{MH} \cdot (1 - \varepsilon)}, \tag{8}$$

where υ_{H_2} is the maximum hydrogen capacity of the tank, and ρ_{H_2} is the density of hydrogen under standard conditions (1 atm, 0 °C), treated as a constant.

2.3. Equilibrium Pressure

The Van't Hoff equation provides a means to determine the equilibrium constant of a reaction across varying temperatures. Gonzatti et al. [13] introduced a modified version of the Van't Hoff equation to estimate the equilibrium pressure:

$$p_{eq,a} = p_0 \cdot e^{\left(\frac{\Delta S_d}{R} - \frac{\Delta H_d}{R \cdot T_t} + (\varphi + \varphi_0)\tan\left[\pi\left(\frac{\rho_s - \rho_{s0}}{\rho_{ss} - \rho_{s0}} - 0.5\right)\right] + \frac{\beta}{2}\right)}, \tag{9}$$

$$p_{eq,d} = p_0 \cdot e^{\left(\frac{\Delta S_d}{R} - \frac{\Delta H_d}{R \cdot T_t} + (\varphi - \varphi_0)\tan\left[\pi\left(\frac{\rho_s - \rho_{s0}}{\rho_{ss} - \rho_{s0}} - 0.5\right)\right] - \frac{\beta}{2}\right)}, \tag{10}$$

where p_0 represents the atmospheric pressure, and ΔH_d and ΔS_d correspond to the enthalpy and entropy changes during desorption, respectively. The parameters φ and φ_0 denote the coefficients related to plateau flatness, while β is the coefficient associated with plateau hysteresis.

2.4. Energy balance

For hydrogen in gas form [22]:

$$\begin{aligned} \upsilon_g \rho_g c_{pg} \frac{dT_g}{dt} &= \upsilon_g \lambda_g \nabla^2 T_g - \rho_g c_{pg} \vec{v} \cdot \nabla T_g \\ &\quad - H_{gs}\left(T_g - T_s\right) A + f_r c_{pg}\left(T_g - T_s\right). \end{aligned} \tag{11}$$

For metal hydride:

$$\begin{aligned} \upsilon_s \rho_s c_{ps} \frac{dT_s}{dt} &= \upsilon_s \lambda_s \nabla^2 T_s + H_{gs}\left(T_g - T_s\right) A \\ &\quad + f_r\left(\frac{\Delta H}{M_{H_2}} + c_{pg} T_s - c_{ps} T_s\right) + Q, \end{aligned} \tag{12}$$

where c_{pg} and c_{ps} are the specific heat of hydrogen and metal hydride, T_g and T_s are the temperature of hydrogen and metal hydride, λ_g and λ_s are the thermal conductivity of hydrogen and metal hydride, A is the exchange area between the gas phase and the solid phase, ΔH is the enthalpy change of reaction (absorption: ΔH_a, desorption: ΔH_d), H_{gs} is the heat transfer coefficient between gas and solid.

The term $\lambda \nabla^2 T$ represents heat conduction, $\rho_g C_{pg} \vec{v} \cdot \nabla T_g$ represents the heat transfer caused by convection, $H_{gs}\left(T_g - T_s\right) A$ represent the natural convection between gas and solid, $f_r c_{pg}\left(T_g - T_s\right)$ is the change of molecular energy and Q is the amount of heat transfer between the ambient and MH tank which has the following form:

$$Q = \frac{k_a (T_a - T_t)}{\upsilon_{MH}}, \tag{13}$$

where k_a is the coefficient and T_a is the ambient temperature.

We assume that the hydrogen gas and metal hydride satisfy local thermal equilibrium, i.e. the temperature of gas T_g is equal to solid T_s ($T_g = T_s = T_t$). Besides, the temperature is distributed uniformly in the tank. Then the two equations (11) and (12) can be simplified and combined into one equation as follows:

$$\begin{aligned} (\upsilon_g \rho_g c_{pg} + \upsilon_s \rho_s c_{ps}) \frac{dT_t}{dt} &= f_r \frac{\Delta H}{M_{H_2}} + f_r T_t (c_{pg} - c_{ps}) \\ &\quad + \frac{k_a (T_a - T_t)}{\upsilon_{MH}}. \end{aligned} \tag{14}$$

2.5. State-space model

The previous model can be rewritten in state-space form as follows:

$$\dot{\mathbf{x}} = \mathbf{f}(\mathbf{x}, u) = \begin{bmatrix} \dfrac{u_1 - f_r\left(x_2, x_3, y_1(x_1, x_3)\right)}{\upsilon_g} \\ \dfrac{f_r\left(x_2, x_3, y_1(x_1, x_3)\right)}{\upsilon_s} \\ \dfrac{f_r \frac{\Delta H}{M_{H_2}} + f_r x_3 (c_{pg} - c_{ps}) + \frac{k_a \cdot (u_2 - x_3)}{\upsilon_{MH}}}{\upsilon_g c_{pg} x_1 + \upsilon_s c_{ps} x_2} \end{bmatrix}, \tag{15}$$

$$\mathbf{y} = \mathbf{h}(\mathbf{x}, u) = \begin{bmatrix} \dfrac{x_1 x_3 R}{M_{H_2}} \\ x_3 \end{bmatrix}, \tag{16}$$

where $\mathbf{x} \in \mathbb{R}^3$ is the state vector, $\mathbf{x} = [\rho_g, \rho_s, T_t]^{\mathrm{T}}$. $\mathbf{u} \in \mathbb{R}^2$ is the input vector, $\mathbf{u} = [f_{in}, T_a]^{\mathrm{T}}$. $\mathbf{y} \in \mathbb{R}^2$ is the output vector, $\mathbf{y} = [p, T_t]^{\mathrm{T}}$.

3. Identifiability analysis of the MH tank

This section analyses the identifiability of the state-space model (15)- (16) of the MH tank model proposed above. As mentioned in the introduction, several methods are available for testing the identifiability of a nonlinear system. However, due to the strong nonlinearity and large scale of the model, only methods for testing local at-a-point identifiability are feasible. Inspired by recent works [26, 27], the correlation method is used in this paper to analyse the identifiability of the model.

3.1. Correlation method

To analyse the local at-a-point identifiability of the nonlinear model, the following general form of the model (15) - (16) is considered:

$$\dot{\mathbf{x}} = \mathbf{f}\left(\mathbf{x}, \mathbf{u}, \boldsymbol{\theta}\right), \tag{17}$$

$$\mathbf{y} = \mathbf{h}(\mathbf{x}, \mathbf{u}, \boldsymbol{\theta}), \tag{18}$$

where $\mathbf{x} \in \mathbb{R}^{n_x}$ denotes the state vector; $\mathbf{u} \in \mathbb{R}^{n_u}$ is the input vector; $\boldsymbol{\theta} = [\boldsymbol{\theta_k}, \boldsymbol{\theta_u}]$ is a constant parameter vector which contains the known parameter vector $\boldsymbol{\theta_k} \in \mathbb{R}^{p_1}$ and unknown parameter vector $\boldsymbol{\theta_u} \in \mathbb{R}^{p_2}$; $\mathbf{f} \in \mathbb{R}^{n_x}$ and $\mathbf{h} \in \mathbb{R}^{n_y}$ are the vector fields.

The correlation method for local at-a-point identifiability relies on analysing the sensitivity of the model outputs at concrete time instants with respect to the parameters. Considering output sensitivity matrix $\mathbf{S} \in \mathbb{R}^{n_y \times p_2 \times n_s}$:

$$\mathbf{S} = \begin{bmatrix} \mathbf{s}\left(t_1\right) \\ \mathbf{s}\left(t_2\right) \\ \vdots \\ \mathbf{s}\left(t_{n_s}\right) \end{bmatrix}, \tag{19}$$

where

$$\mathbf{s}\left(t_i\right) = \begin{bmatrix} s_{11}\left(t_i\right) & \dots & s_{1p_2}\left(t_i\right) \\ \vdots & \ddots & \vdots \\ s_{n_y1}\left(t_i\right) & \dots & s_{n_yp_2}\left(t_i\right) \end{bmatrix}, \tag{20}$$

and the elements of $\mathbf{s}\left(t_i\right)$ are named the sensitivity coefficients. For the nominal parameter vector $\boldsymbol{\theta_u}^*$, given system initial conditions $\mathbf{x_0}$ and time instants t_k with $k \in \{1, \cdots, n_s\}$, the elements of $s\left(t_i\right)$ are defined as

$$s_{ij}\left(t_k\right) = \frac{\partial y_i\left(t_k, \boldsymbol{\theta_u}^*, \mathbf{x_0}\right)}{\partial \theta_{u,j}} \tag{21}$$

with $i \in \{1, \cdots, n_y\}$ and $j \in \{1, \cdots, p_2\}$. y_i and $\theta_{u,j}$ are the elements of output vector $\mathbf{y}$ and unknown parameter vector $\boldsymbol{\theta_u}$, respectively.

The main idea of the correlation method is to study the linear dependence of any two columns $\mathbf{S}_{.i}, \mathbf{S}_{.j} \in \mathbb{R}^{n_y \times n_s}$ of output sensitivity matrix $\mathbf{S}$. The linear dependence of any two columns $\mathbf{S}_{.i}, \mathbf{S}_{.j}$ can be obtained by calculating the sample correlation between $\mathbf{S}_{.i}$ and $\mathbf{S}_{.j}$

$$\operatorname{corr}\left(\mathbf{S}_{.i}, \mathbf{S}_{.j}\right) = \frac{\operatorname{cov}\left(\mathbf{S}_{.i}, \mathbf{S}_{.j}\right)}{\sigma\left(\mathbf{S}_{.i}\right)\sigma\left(\mathbf{S}_{.j}\right)}, \tag{22}$$

where $\operatorname{cov}\left(\mathbf{S}_{.i}, \mathbf{S}_{.j}\right)$ is the sample covariance between $\mathbf{S}_{.i}$ and $\mathbf{S}_{.j}$, $\sigma(\cdot)$ is the standard deviation. Then for the whole matrix $\mathbf{S}$ and (22), a matrix $\mathbf{C}$, which includes the absolute correlation values between columns of $\mathbf{S}$ exceeding the threshold $1 - \epsilon_c$, can be computed as

$$\mathbf{C} = \begin{bmatrix} \operatorname{corr}^*\left(\mathbf{S}_{.1}, \mathbf{S}_{.1}\right) & \dots & \operatorname{corr}^*\left(\mathbf{S}_{.1}, \mathbf{S}_{.p_2}\right) \\ \vdots & \ddots & \vdots \\ \operatorname{corr}^*\left(\mathbf{S}_{.p_2}, \mathbf{S}_{.1}\right) & \dots & \operatorname{corr}^*\left(\mathbf{S}_{.p_2}, \mathbf{S}_{.p_2}\right) \end{bmatrix}, \tag{23}$$

where $\epsilon_c \in [0, 1]$ is a tunable parameter and

$$\operatorname{corr}^*\left(\mathbf{S}_{.i}, \mathbf{S}_{.j}\right) = \begin{cases} \left|\operatorname{corr}\left(\mathbf{S}_{.i}, \mathbf{S}_{.j}\right)\right|, & \left|\operatorname{corr}\left(\mathbf{S}_{.i}, \mathbf{S}_{.j}\right)\right| \geq 1 - \epsilon_c, & \text{(24a)} \\ 0, \text{ else.} & & \text{(24b)} \end{cases}$$

Based on matrix $\mathbf{C}$, the total correlation of each parameter c_i^{tot} can be calculated as

$$c_i^{tot} = \sum_{j \in \boldsymbol{\theta_u}, j \neq i} \mathbf{C}_{i,j}. \tag{25}$$

The value of the total correlation indicates the level of identifiability of the parameter, if there exist two parameters with the same total correlation, adjust the parameter ϵ_c until the total correlation is different. However, if the same total correlation of any two parameters can not be different by tuning ϵ_c, it indicates that two parameters with the same total correlation can not be identified.

The correlation method of identifiability for the MH tank is presented in Algorithm 1. Through a comparison of the total correlation for each parameter, it is feasible to discern the level of identifiability for each parameter. It is important to highlight that a higher total correlation of a parameter corresponds to less identification. Conversely, a lower total correlation indicates more identification.

3.2. Result of identifiability analysis

To facilitate the identifiability analysis, one operating profile corresponding to the mixed charge and discharge of the MH tank is defined.

In the MH tank model (15) - (16) proposed in the above section, the unknown parameter vector is $\boldsymbol{\theta_u} = [\Delta H_a, \Delta S_d, \Delta H_d, \varphi, \varphi_0, \beta, c_a, c_d, E_a, E_d, k_a, c_{ps}, \rho_{s0}, \epsilon, \upsilon_{MH}]$. The prespecified values of unknown parameters $\boldsymbol{\theta_u}$ used for identifiability analysis are shown in Table 1. Other parameters used in the model are listed in Table 2. The initial conditions of the defined profile are defined as $\rho_g(t_0)$=0.9759 kg/m^3 and $\rho_s(t_0) = 6270\,\text{kg/m}^3$. To fully consider the charge and discharge scenarios, an extreme case has been chosen, i.e. the normalized mass-flow rate is a periodic square wave signal. $f_{in} = 0\,\text{kg/m}^3\text{/s}$ while $t \in$

Algorithm 1: Correlation method of identifiability for the MH tank

Input : Normalized mass-flow rate f_{in}, Ambient temperature T_a

Initialization:

- Set the initial value of the hydrogen and metal-hydride density $\rho_g(t_0)$, $\rho_s(t_0)$
- Set the prespecified parameter values (either nominal or actual estimates) of each parameter θ_j
- Set the sampling interval Δt and the stop time t_{n_s}

Start procedure;
Compute $t_1 = t_0 + \Delta t$;
while $t_k \leq t_{n_s}$ **do**
    Compute the output sensitivity matrix **S** via (19);
    Compute the matrix **C** via (23);
    Compute the total correlation c_i^{tot} of each parameter by (25);
    Set $t_{k+1} = t_k + \Delta t$;
    Set $k = k + 1$;
end
End procedure;
Output: Total correlation c_i^{tot}

$[0, 600s)$, then increases by $0.001\,\mathrm{kg/m^3/s}$ in steps every 600s. f_{in} decreases to $0\,\mathrm{kg/m^3/s}$ while $t \in [1800s, 2400s)$, then decreases by $0.001\,\mathrm{kg/m^3/s}$ in steps every 600s and increases to $0\,\mathrm{kg/m^3/s}$ while $t \in [3600s, 4200s)$. Fig.1 shows the system dynamics for the mixed charging & discharging process.

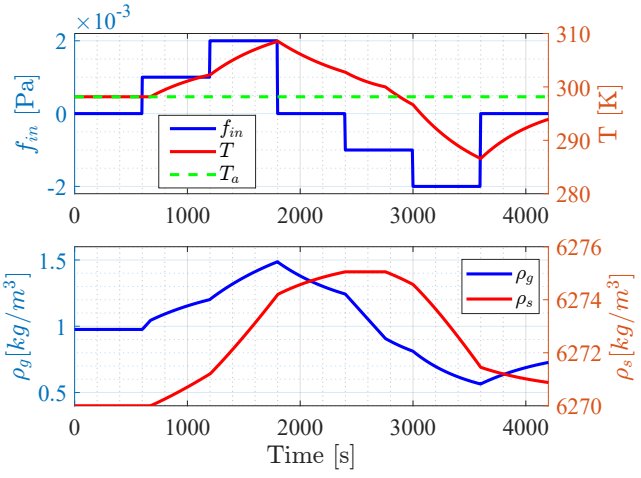

Fig. 1- The mixed charging & discharging profile of sensitivity analysis.

Setting $\epsilon_c = 0.3$, we can calculate the matrix C and the total correlation c_i^{tot} based on the defined operating profile. The result of the total correlation c_i^{tot} for each parameter is shown in Table 3. It can be observed that each parameter in the model has a different total correlation, which indicates that each parameter is identifiable. In addition, the total correlation reflects the level of identifiability of the parameters. The order of identifiability of the parameters from higher to lower is: E_d, c_d, c_{ps}, k_a, φ_0, β, ΔH_d, ΔS_d, φ, E_a, c_a, ρ_{s0}, ϵ, ΔH_a, υ_{MH}.

4. Sensitivity analysis of the MH tank

This section analyses the parametric sensitivity of the state-space model (15) - (16) of the MH tank proposed above. Based on the result of the analysis in the above section, each parameter can be identified using the output information. However, the model contains 15 parameters that need to be calibrated, and the direct use of parameter identification methods such as the PSO algorithm has a huge computational cost. To reduce the number of unknown parameters that need to be calibrated, it is necessary to analyse the sensitivity of the parameters. When the parameter identification is carried out, the unknown parameters with higher sensitivity are identified in priority, and for those unknown parameters with lower sensitivity, reasonable values can be selected based on the results of the existing literature.

The method used in this paper to analyse the sensitivity of the model parameters is the FOTSA method, which is described in detail in our previous work [5] and will not be repeated in this paper. The main idea of FOTSA is to calculate the sensitivity index s_i for each parameter during the sample time. Larger sensitivity index means that the parameter has higher sensitivity to the system trajectory. In this section, using the same sample time, prespecified values of unknown parameters, and other model parameters as in the identifiability analysis in the previous section, the sensitivity indexes for each parameter are calculated for a 1% variation in comparison to the prespecified values. The results are shown in Table 4. The sensitivity of each parameter with respect to ρ_g, ρ_s, T_t is ranked according to the value of the sensitivity index and the results are shown in Table 5.

5. Multi-objective parameter identification from data

This section uses the paretosearch algorithm (also a command in Matlab for multi-objective optimisation) to identify the unknown parameters in the state-space model. Since the model developed contains two outputs, we first use the single objective and PSO algorithm to identify the unknown parameters. Secondly, the unknown parameters are identified using the multi-objective and paretosearch algorithms. The results show that multi-objective identification performs better than single-objective identification.

5.1. Single objective identification with PSO algorithm

In the state-space model (15) - (16), two outputs, p and T_t, can be measured directly from sensors. Considering tank pressure p as a single-objective optimisation variable, the

Table 1
Prespecified values of parameters [2, 4, 9, 16, 28]

Parameter	Symbol	Prespecified value	Unit
Entropy change for absorption	ΔH_a	22540	J/mol
Entropy change for desorption	ΔS_d	111.77	J/(mol · K)
Enthalpy change for desorption	ΔH_d	26680	J/mol
Plateau flatness coefficient	φ	0.1843	-
Plateau flatness coefficient	φ_0	0.0042	-
Plateau hysteresis coefficient	β	0.2355	-
Absorption constant	c_a	3928.1	1/s
Desorption constant	c_d	4952.2	1/s
Activation energy for absorption	E_a	38236	J/mol
Activation energy for desorption	E_d	30915	J/mol
Heat transfer coefficient	k_a	0.7	J/(K · s)
Specific heat of MH	c_{ps}	400	J/(kg · K)
Density of the metal alloy	ρ_{s0}	6211.1	kg/m^3
Porosity of the MH	ϵ	0.6997	-
Volume of MH	v_{MH}	$0.353 \cdot 10^{-3}$	m^3

Table 2
Other parameters used in the MH tank model [15]

Symbol	Value	Symbol	Value
v_{H_2}	0.35 m^3	ρ_{H_2}	0.0897 kg/m^3
R	8.314 J/(mol · K)	p_0	101 325 Pa
M_{H_2}	$2.016 \cdot 10^{-3}$kg/mol	T_a	298.15 K
v_{tank}	$0.48 \cdot 10^{-3}$m^3	c_{pg}	14890J/(kg · K)

Table 3
Total correlation c_i^{tot} for each parameter

Parameter	Symbol	c^{tot}
Entropy change for absorption	ΔH_a	9.2755
Entropy change for desorption	ΔS_d	6.4480
Enthalpy change for desorption	ΔH_d	5.7043
Plateau flatness coefficient	φ	7.1298
Plateau flatness coefficient	φ_0	5.1297
Plateau hysteresis coefficient	β	5.1442
Absorption constant	c_a	7.1658
Desorption constant	c_d	1.7348
Activation energy for absorption	E_a	7.1619
Activation energy for desorption	E_d	1.7330
Heat transfer coefficient	k_a	4.8636
Specific heat of metal hydride	c_{ps}	3.0355
Density of the metal alloy	ρ_{s0}	7.1797
Porosity of the metal hydride	ϵ	7.9023
Volume of the metal hydride	v_{MH}	9.4810

following single-objective optimisation problem can be constructed, where the objective function is the mean magnitude of relative error (MMRE):

$$\min_{\boldsymbol{\theta}} f_1(\mathbf{x}, \mathbf{u}, \boldsymbol{\theta}) \tag{26}$$

$$f_1(\mathbf{x}, \mathbf{u}, \boldsymbol{\theta}) = \frac{1}{N} \cdot \sum_{t=0}^{t=N\Delta t} \left| \frac{\left(p(t) - p_{exp}(t)\right)}{p_{exp}(t)} \right| \tag{27}$$

$$s.t. \quad \underline{\boldsymbol{\theta}} \le \boldsymbol{\theta} \le \overline{\boldsymbol{\theta}}, \tag{28}$$

where p_{exp} is the experimental data of tank pressure, $\underline{\boldsymbol{\theta}}$ and $\overline{\boldsymbol{\theta}}$ are the lower and upper bounds of $\boldsymbol{\theta}$, Δt is the sampling interval, and N is the number of sampling times of the whole experiment. The standard PSO method [17] is employed to seek optimum values for the unknown parameters. Table 6 presents the search range of unknown parameters for the PSO method.

An experiment is performed using the real setup depicted in Fig. 2. The experimental setup primarily consists of a

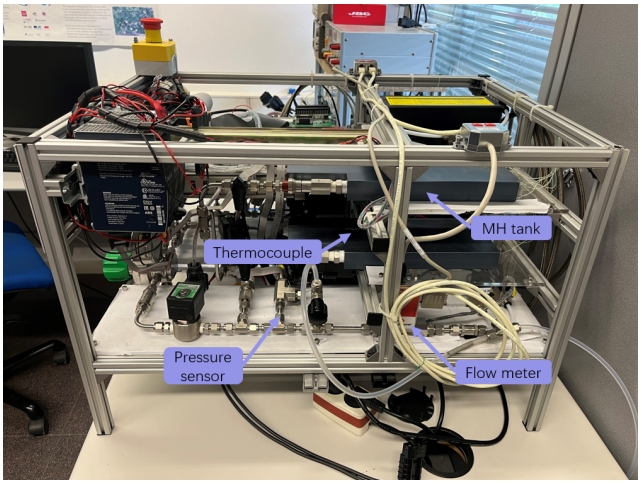

Fig. 2- View of the MH tank test bench environment.

commercial metal hydride (MH) tank (H2planet® MyH2

Table 4
Sensitivity index for $\rho_g(s_1)$, $\rho_s(s_2)$, $T_t(s_3)$ with 1% parameter variation

Parameter	Symbol	s_1	s_2	s_3
Entropy change for absorption	ΔH_a	0.0241	0.0852	0.5531
Entropy change for desorption	ΔS_d	1.6572	5.8465	16.6794
Enthalpy change for desorption	ΔH_d	1.2902	4.5520	13.3477
Plateau flatness coefficient	φ	0.0292	0.1031	0.3169
Plateau flatness coefficient	φ_0	$6.6576 \cdot 10^{-4}$	0.0023	0.0156
Plateau hysteresis coefficient	β	0.0145	0.0512	0.3479
Absorption constant	c_a	$6.3517 \cdot 10^{-4}$	0.0022	0.0056
Desorption constant	c_d	$1.2344 \cdot 10^{-4}$	$4.3551 \cdot 10^{-4}$	0.0011
Activation energy for absorption	E_a	0.0095	0.0335	0.0850
Activation energy for desorption	E_d	0.0016	0.0056	0.0146
Heat transfer coefficient	k_a	0.0257	0.0906	0.6400
Specific heat of metal hydride	c_{ps}	0.0119	0.0418	0.5119
Density of the metal alloy	ρ_{s0}	4.0809	14.3975	45.1059
Porosity of the metal hydride	ϵ	0.0968	0.3416	1.0058
Volume of the metal hydride	v_{MH}	0.0662	0.2337	0.7508

Table 5
Rank of sensitivity indexes for each parameter

Sensitivity index	1	2	3	4	5	6	7	8	9	10	11	12	13	14	15
s_1	ρ_{s0}	ΔS_d	ΔH_d	ϵ	v_{MH}	φ	k_a	ΔH_a	β	c_{ps}	E_a	E_d	φ_0	c_a	c_d
s_2	ρ_{s0}	ΔS_d	ΔH_d	ϵ	v_{MH}	φ	k_a	ΔH_a	β	c_{ps}	E_a	E_d	φ_0	c_a	c_d
s_3	ρ_{s0}	ΔS_d	ΔH_d	ϵ	v_{MH}	k_a	ΔH_a	c_{ps}	β	φ	E_a	φ_0	E_d	c_a	c_d

Table 6
PSO search range of the unknown parameters for MH tank [2, 4, 9, 16, 28]

Parameter	Lower	Upper	Unit
ΔH_a	20000	23000	J/mol
ΔS_d	109	113	J/(mol · K)
ΔH_d	25000	32000	J/mol
φ	0	2	-
φ_0	0	1	-
β	0	2	-
c_a	10	5000	1/s
c_d	10	5000	1/s
E_a	30000	50000	J/mol
E_d	30000	50000	J/mol
k_a	0.1	30	J/(K · s)
c_{ps}	300	7000	J/(kg · K)
ρ_{s0}	6200	6400	kg/m^3
ϵ	0.1	0.7	-
v_{MH}	$0.3 \cdot 10^{-3}$	$0.48 \cdot 10^{-3}$	m^3

SLIM 350), mass-flow meters (F-111B), pressure sensors (PR-21Y), and thermocouples. All sensors are integrated with a real-time data acquisition platform (NI sbRIO 9629) to facilitate data storage and processing. The experiment is divided into two phases: charging and discharging. Fig. 3 illustrates the input data collected during the experiment. The relationship between the flow rate F_{in} and the normalized mass-flow rate f_{in} is described by the following equation:

$$F_{in} = \frac{f_{in} \cdot v_{MH} \cdot 60 \cdot 22.4}{M_{H2}}. \tag{29}$$

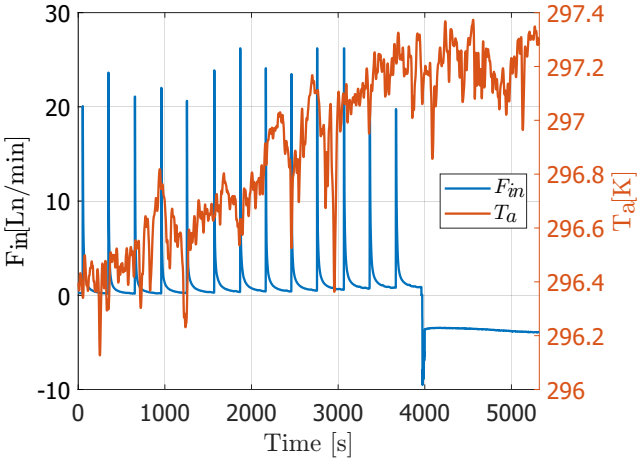

Fig. 3- Experimental inputs

Subsequently, we minimize the single objective function (28) using the PSO algorithm and reproduce the model with the optimal values. The comparison between model outputs and experimental data is shown in Fig. 4 and Fig. 5. It can be observed from these two figures that the calibrated result of p is good but the calibrated result of T_t seems not so good. This

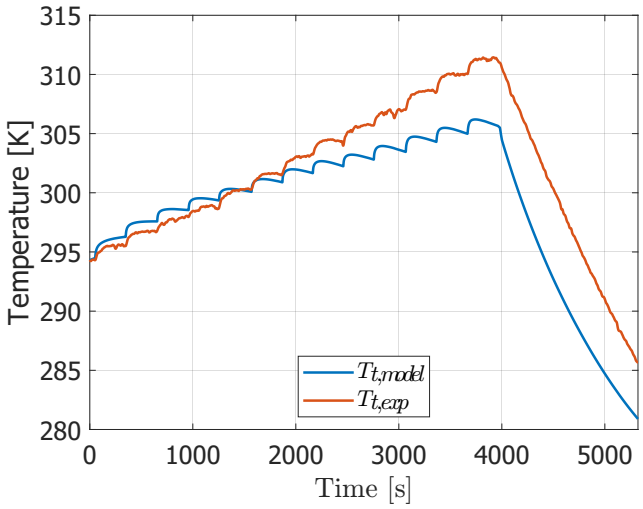

Fig. 4- Comparison between model temperature and experimental temperature with single object identification

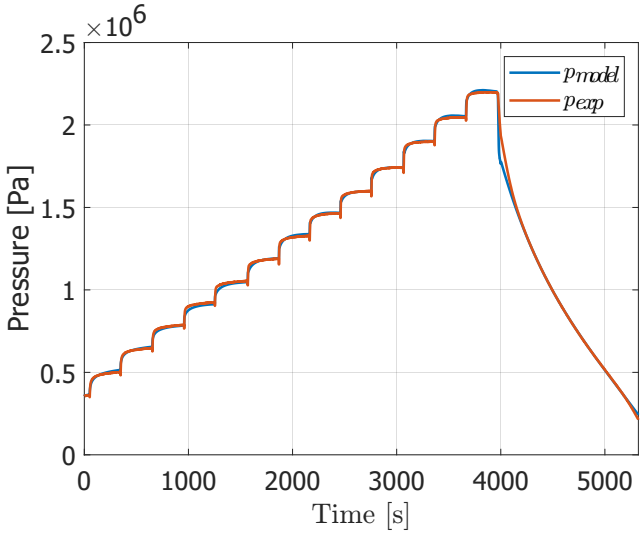

Fig. 5- Comparison between model tank pressure and experimental tank pressure with single object identification

is because the single-objective function we constructed only considers the error in p. To describe the identification results of the unknown parameters more intuitively, the optimal values with single object identification and the corresponding objective function value are listed in Table 7. The second objective function f_2 can be expressed as:

$$f_2(\mathbf{x}, \mathbf{u}, \theta) = \frac{1}{N} \cdot \sum_{t=0}^{t=N\Delta t} \left| \frac{\left(T_t(t) - T_{t,exp}(t)\right)}{T_{t,exp}(t)} \right| \tag{30}$$

where $T_{t,exp}$ is the experimental data of tank temperature.

5.2. Multi-objective identification with paretosearch algorithm

In contrast to the previous subsection, to utilise the error information of the tank pressure p and temperature T_t, both are considered as multi-objective optimisation variables.

Table 7
Optimal values with single object identification and the corresponding objective function value

Parameter	Value	Unit
ΔH_a	20257	J/mol
ΔS_d	112.5369	J/(mol · K)
ΔH_d	26141	J/mol
φ	0.3601	-
φ_0	0.0187	-
β	0.1707	-
c_a	2697.4	1/s
c_d	4813.8	1/s
E_a	31458	J/mol
E_d	33119	J/mol
k_a	3.2511	J/(K · s)
c_{ps}	5439.8	J/(kg · K)
ρ_{s0}	6399.9	kg/m^3
ϵ	0.6975	-
v_{MH}	$3.1236 \cdot 10^{-4}$	m^3
f_1	0.0089	
f_2	0.0104	

The following multi-objective optimisation problem can be constructed, where the objective function is still based on the MMRE:

$$\min_{\theta} \left[f_1(\mathbf{x}, \mathbf{u}, \theta), f_2(\mathbf{x}, \mathbf{u}, \theta) \right] \tag{31}$$

$$s.t. \quad \underline{\theta} \le \theta \le \overline{\theta}, \tag{32}$$

The same experimental data as in the previous subsection, along with the paretosearch algorithm [11], are used to solve the problem. To speed up the solving process and help the solver find better solutions, the points that minimize the individual objective functions—i.e., the parameter values in Table 7—are used as initial points. Fig. 6 shows the Pareto front of the multi-objective problem.

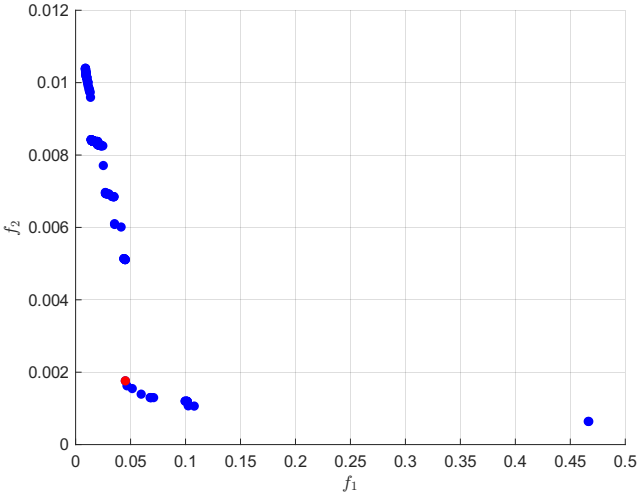

Fig. 6- Pareto front of optimal solutions (f_1: MMRE of the tank pressure; f_2: MMRE of the tank temperature; Red point: the selected optimal solution)

In practice, every solution on the Pareto front is optimal, and the choice of a point depends entirely on the objective that the decision-maker prioritizes. Inspired by [24], the decision-making method Linear Programming for Multidimensional Analysis of Preference (LINMAP) [21] is adopted in this paper to select the best optimal solution from the Pareto front. Specifically, in our case, the ideal solution $f_{ideal} = \left(f_{1,min}, f_{2,min}\right)$ is first built based on the two endpoints of the Pareto front, i.e., the optimal point of the single objective. Then, the Euclidean distance D_i between the points on the Pareto front and the ideal point is calculated as follows:

$$D_i = \sqrt{\sum_{j=1}^{2} w_j \left(f_{i,j} - f_{j,min}\right)^2} \tag{33}$$

where i is the index of solution points on the Pareto front, j is the objective index in the objective space ($j = 1, 2$) and w_j is the weight factor of the objective f_j. In our case, we consider that calibrating the pressure and temperature of the tank are equally important and the weights should be the same. However, it should be noted that in the objective space, f_1 and f_2 are of different orders of magnitude, so f_1 needs to be scaled before calculating the Euclidean distance. Therefore, the weights are set to $w_1 = 0.1$ and $w_2 = 1$. Based on the calculated Euclidean distance of each point from the ideal point, the point with the minimum distance is selected. The comparison between model outputs and experimental data is shown in Fig. 7 and Fig. 8. Compared to the results of

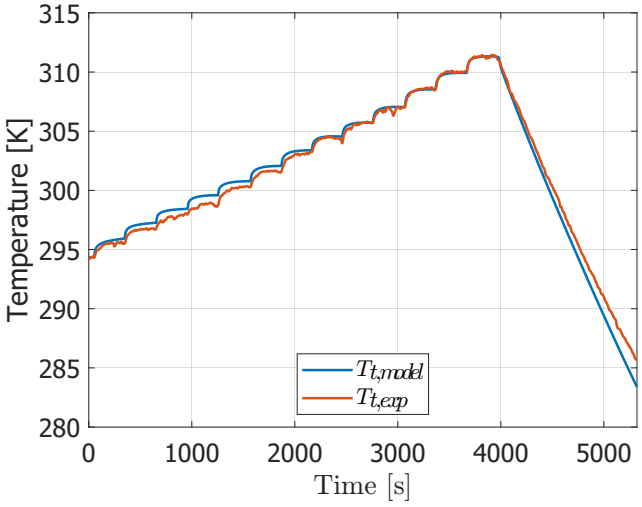

Fig. 7- Comparison between model temperature and experimental temperature with multi-object identification

the single-objective optimisation in the previous subsection, it can be seen that the multi-objective optimisation method balances the two objectives. The optimal values from multi-object identification and the corresponding objective function values are listed in Table 8.

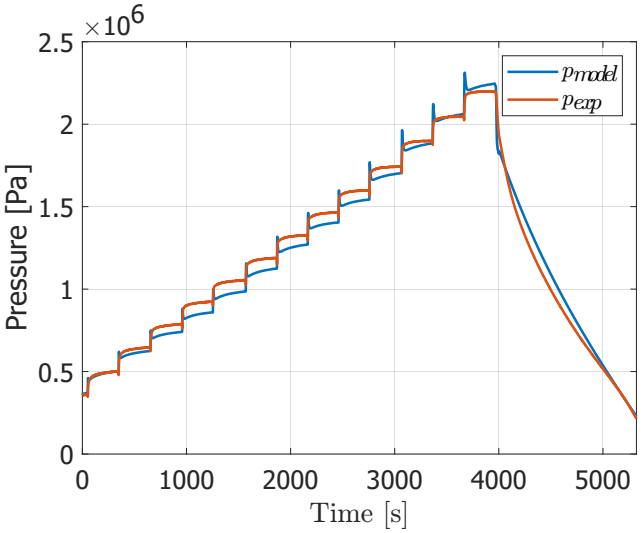

Fig. 8- Comparison between model tank pressure and experimental tank pressure with multi-object identification

Table 8
Optimal values with multiobject identification and the corresponding objective function value

Parameter	Value	Unit
ΔH_a	20000	J/mol
ΔS_d	109	J/(mol · K)
ΔH_d	25530	J/mol
φ	0.3228	-
φ_0	0	-
β	0.1333	-
c_a	388.6084	1/s
c_d	2761.0	1/s
E_a	30847	J/mol
E_d	32507	J/mol
k_a	1.2138	J/(K · s)
c_{ps}	6425.6	J/(kg · K)
ρ_{s0}	6247.0	kg/m^3
ϵ	0.6928	-
v_{MH}	$3 \cdot 10^{-4}$	m^3
f_1	0.0045	
f_2	0.0018	

6. Conclusions and future work

In this study, a three-dimensional state-space model of the MH tank is proposed and analysed. The identifiability analysis demonstrates that the model allows for the determination of a unique parameter vector based on output information. To address the computational challenges posed by the large number of unknown parameters, a sensitivity analysis is performed, effectively reducing the parameter set to be identified. By comparing single-objective and multi-objective identification methods using the same experimental data, it is found that the multi-objective approach yields better results.

Nomenclature

Abbreviations

MH	Metal hydride
PCT	Pressure-Composition-Temperature
FOTSA	First-order Trajectory Sensitivity Analysis

Parameters

ρ_g	Density of hydrogen (kg/m^3)
m'_{in}	Mass flow rate of hydrogen (kg/s)
m'_r	Mass flow rate of hydrogen sorption (kg/s)
v_t	Volume of tank (m^3)
v_{MH}	Volume of MH (m^3)
ε	Porosity of MH
f_{in}	Normalized mass flow rate of hydrogen ($kg/m^3/s$)
f_r	Normalized sorption mass flow rate of hydrogen ($kg/m^3/s$)
v_g	Normalized volume of hydrogen
ρ_s	Density of the MH (kg/m^3)
v_s	Normalized volume of the MH
c_a	Absorption constant ($1/s$)
c_d	Desorption constant ($1/s$)
E_a	Ectivation energy of absorption (J/mol)
E_d	Ectivation energy of desorption (J/mol)
$p_{eq,a}$	Equilibrium pressure of absorption (Pa)
$p_{eq,d}$	Equilibrium pressure of desorption (Pa)
R	Universal gas constant ($8.314\,J/mol/K$)
T_t	Tank temperature (K)
ρ_{ss}	Saturated density of MH with complete absorption of hydrogen (kg/m^3)
ρ_{s0}	Empty density of the MH without any hydrogen (kg/m^3)
p	Pressure of hydrogen (Pa)
M_{H_2}	Molar mass of hydrogen ($2.016 \times 10^{-3}\,kg/mol$)
v_{H_2}	Maximum volume of hydrogen that can be absorbed (m^3)
ρ_{H_2}	Density of hydrogen in standard state (kg/m^3)
p_0	Atmospheric pressure (101 325 Pa)
ΔS_d	Entropy change for desorption ($J/mol/K$)
ΔH_d	Enthalpy change for desorption (J/mol)
ΔH_a	Enthalpy change for absorption (J/mol)
φ, φ_0	Plateau flatness coefficients
β	Plateau hysteresis coefficient
F_{in}	Flow rate of hydrogen (Ln/min)
Q	Heat exchange per unit volume from the ambient air to the MH tank (W/m^3)
c_{pg}	Specific heat of hydrogen ($J/(kg\,K)$)
c_{ps}	Specific heat of MH ($J/(kg\,K)$)

Subscripts

a	Absorption
d	Desorption

Acknowledgement

This work is part of the Project MAFALDA (PID2021-126001OB-C31 funded by MCIN/ AEI /10.13039/501100011033 and by "ERDF A way of making Europe") and Project MASHED (TED2021-129927B-I00 funded by MCIN/AEI /10.13039/501100011033 and by the "European Union Next GenerationEU/PRTR").

This work is partially supported by the National Natural Science Foundation of China under grant (62273169) and the Chinese Scholarship Council (CSC) under grant (202208530009).

References

[1] Askri, F., Salah, M.B., Jemni, A., Nasrallah, S.B., 2009. Heat and mass transfer studies on metal-hydrogen reactor filled with mmni4. 6fe0. 4. international journal of hydrogen energy 34, 6705–6711.

[2] Barale, J., Nastro, F., Violi, D., Rizzi, P., Luetto, C., Baricco, M., 2023. A metal hydride compressor for a small scale h2 refuelling station. International Journal of Hydrogen Energy .

[3] Benchluch, S.M., Chow, J.H., 1993. A trajectory sensitivity method for the identification of nonlinear excitation system models. IEEE Transactions on Energy Conversion 8, 159–164.

[4] Capurso, G., Schiavo, B., Jepsen, J., Lozano, G., Metz, O., Saccone, A., De Negri, S., Bellosta von Colbe, J.M., Klassen, T., Dornheim, M., 2016. Development of a modular room-temperature hydride storage system for vehicular applications. Applied Physics A 122, 1–11.

[5] Chen, M., Batlle, C., Escachx, B., Costa-Castelló, R., Na, J., 2024. Sensitivity analysis and calibration for a two-dimensional state-space model of metal hydride storage tanks based on experimental data. Journal of Energy Storage 94, 112316.

[6] Choi, H., Mills, A., 1990. Heat and mass transfer in metal hydride beds for heat pump applications. International Journal of Heat and Mass Transfer 33, 1281–1288.

[7] Choi, J., Harvey, J.W., Conklin, M.H., 1999. Use of multi-parameter sensitivity analysis to determine relative importance of factors influencing natural attenuation of mining contaminants, in: Proceedings of the Toxic Substances Hydrology Program Meeting, Charleston, SC, pp. 185–192.

[8] Christopher Frey, H., Patil, S.R., 2002. Identification and review of sensitivity analysis methods. Risk analysis 22, 553–578.

[9] Chung, C., Lin, C.S., 2009. Prediction of hydrogen desorption performance of mg2ni hydride reactors. International Journal of Hydrogen Energy 34, 9409–9423.

[10] Correa, J.M., Farret, F.A., Popov, V.A., Simoes, M.G., 2005. Sensitivity analysis of the modeling parameters used in simulation of proton exchange membrane fuel cells. IEEE Transactions on energy conversion 20, 211–218.

[11] Custódio, A.L., Madeira, J.A., Vaz, A.I.F., Vicente, L.N., 2011. Direct multisearch for multiobjective optimization. SIAM Journal on Optimization 21, 1109–1140.

[12] Degenring, D., Froemel, C., Dikta, G., Takors, R., 2004. Sensitivity analysis for the reduction of complex metabolism models. Journal of

Process Control 14, 729–745.
[13] Gonzatti, F., Miotto, M., Farret, F., 2018. Automation and analysis of the operation of (la0. 85ce0. 15) ni5 in energy storage plants. international journal of hydrogen energy 43, 2850–2860.
[14] Jacquez, J.A., Greif, P., 1985. Numerical parameter identifiability and estimability: Integrating identifiability, estimability, and optimal sampling design. Mathematical Biosciences 77, 201–227.
[15] Keow, A.L.J., Mayhall, A., Cescon, M., Chen, Z., 2021. Active disturbance rejection control of metal hydride hydrogen storage. International Journal of Hydrogen Energy 46, 837–851.
[16] Kölbig, M., Bürger, I., Linder, M., 2019. Characterization of metal hydrides for thermal applications in vehicles below 0° c. International Journal of Hydrogen Energy 44, 4878–4888.
[17] Li, Q., Chen, W., Wang, Y., Liu, S., Jia, J., 2010. Parameter identification for pem fuel-cell mechanism model based on effective informed adaptive particle swarm optimization. IEEE Transactions on Industrial Electronics 58, 2410–2419.
[18] MacDonald, B.D., Rowe, A.M., 2006. Impacts of external heat transfer enhancements on metal hydride storage tanks. International Journal of Hydrogen Energy 31, 1721–1731.
[19] Mayer, U., Groll, M., Supper, W., 1987. Heat and mass transfer in metal hydride reaction beds: experimental and theoretical results. Journal of the Less Common Metals 131, 235–244.
[20] Miao, H., Xia, X., Perelson, A.S., Wu, H., 2011. On identifiability of nonlinear ode models and applications in viral dynamics. SIAM review 53, 3–39.
[21] Mostafavi, S.A., Hajabdollahi, Z., Ilinca, A., 2022. Multi-objective optimization of metal hydride hydrogen storage tank with phase change material. Thermal Science and Engineering Progress 36, 101514.
[22] Nasrallah, S.B., Jemni, A., 1997. Heat and mass transfer models in metal-hydrogen reactor. International Journal of Hydrogen Energy 22, 67–76.
[23] Nield, D.A., Bejan, A., et al., 2006. Convection in porous media. volume 3. Springer.
[24] Nyamsi, S.N., Tolj, I., Pasupathi, S., 2023. Multi-objective optimization of a metal hydride reactor coupled with phase change materials for fast hydrogen sorption time. Journal of energy storage 71, 108089.
[25] Qian, J., Sun, X., Zhong, X., Zeng, J., Xu, F., Zhou, T., Shi, K., Li, Q., 2024. Multi-objective optimization design of the wind-to-heat system blades based on the particle swarm optimization algorithm. Applied Energy 355, 122186.
[26] Quaiser, T., Mönnigmann, M., 2009. Systematic identifiability testing for unambiguous mechanistic modeling–application to jak-stat, map kinase, and nf-κ b signaling pathway models. BMC systems biology 3, 1–21.
[27] Sanz Bermejo, F., Ramirez-Laboreo, E., Sagüés Blázquiz, C., et al., 2023. Análisis de identificabilidad estructural de un sistema de transferencia de calor. Revista Iberoamericana de Automática e Informática Industrial 20, 412–420.
[28] Skripnyuk, V., Ron, M., 1999. Evaluation of kinetics by utilizing the normalized pressure dependence method for the alloy ti0. 95zr0. 05mn1. 48v0. 43fe0. 08al0. 01. Journal of Alloys and Compounds 293, 385–390.
[29] Suárez, S.H., Chabane, D., N'Diaye, A., Ait-Amirat, Y., Elkedim, O., Djerdir, A., 2022. Evaluation of the performance degradation of a metal hydride tank in a real fuel cell electric vehicle. Energies 15, 3484.
[30] Suda, S., Kobayashi, N., Yoshida, K., 1980. Reaction kinetics of metal hydrides and their mixtures. Journal of the Less Common Metals 73, 119–126.
[31] Vajda, S., Rabitz, H., Walter, E., Lecourtier, Y., 1989. Qualitative and quantitative identifiability analysis of nonlinear chemical kinetic models. Chemical Engineering Communications 83, 191–219.
[32] Xiao, J., Zeng, X., Chen, H., Yang, L., 2023. An investigation into the multi-parameter identification and model optimization strategy of the pct curves of hydrogen storage alloys by multiple intelligent algorithms. International Journal of Hydrogen Energy 48, 1943–1955.
[33] Yue, H., Brown, M., Knowles, J., Wang, H., Broomhead, D.S., Kell, D.B., 2006. Insights into the behaviour of systems biology models from dynamic sensitivity and identifiability analysis: a case study of an nf-κb signalling pathway. Molecular BioSystems 2, 640–649.